Surface electronic structure of Mg(0001)

U. O. Karlsson, G. V. Hansson, P. E. S. Persson, and S. A. Flodström
Department of Physics and Measurement Technology, Linköping Institute of Technology, S-581 83 Linköping, Sweden
(Received 8 February 1982)

Mg(0001) has been studied with angle-resolved photoemission spectroscopy for photon energies in the range 7.0–26.8 eV. The polar-angle dependence of the photoelectron emission was recorded along the two symmetry lines $\bar{\Gamma}\bar{M}$ and $\bar{\Gamma}\bar{K}$ of the surface Brillouin zone. Six structures are identified in the spectra. Two sharp peaks are assigned to emission from surface states. One is located in a band gap around $\bar{\Gamma}$, the other in a band gap near $\bar{M}$. Three peaks are interpreted as indirect transitions from different electron pockets in the Brillouin zone. These regions with high densities of occupied states are located close to Γ, L, and K in the bulk Brillouin zone. Our experiments confirm earlier magnetoacoustic attenuation and de Haas–van Alphen experiments with respect to these electron pockets. Finally one broad structure is interpreted as a direct optical transition between bulk bands.

INTRODUCTION

Magnesium and aluminum are considered to be two of the most free-electron-like metals. The bulk crystal potential is weak in these metals and we expect the photoemission spectra to be dominated by structures excited by surface photoemission at photon energies below the plasmon energy.[1–3] For Al a number of photoemission studies[4–6] verified these theories. For example, the predicted surface state and surface resonances in the band gap projected from the X point[7–10] were experimentally established by angle-resolved ultraviolet photoelectron spectroscopy (ARUPS) on the (100), (110), and (111) crystal faces[4–6] of aluminum.

Clearly both Al and Mg have weak periodic potentials, but the fact that energy band gaps exist in both metals indicates that the electron structure is not entirely free-electron-like. We can therefore expect that bulk photoemission will contribute to the photocurrent. Recent ARUPS experiments on Al (Refs. 11 and 12) have also shown that bulk photoemission, in terms of direct optical transitions, are of significance.

No ARUPS studies have been reported to our knowledge for Mg single-crystal surfaces. A possible explanation might be the extreme reactivity to oxygen for Mg.[13] Mg reacts a factor of 100 faster with oxygen as compared to Al. We should also note that for photon energies above the bulk-plasmon energy (10.5 eV), the photoemission cross section is very small.[1,6]

We have performed an ARUPS study of the Mg(0001) crystal face utilizing photon energies in the range 7.0–26.8 eV. The angle of electron emission has been varied to probe electron states in the two symmetry planes ΓALM and ΓAHK or in terms of the two-dimensional surface Brillouin zone (2D SBZ) along the symmetry lines $\bar{\Gamma}\bar{M}$ and $\bar{\Gamma}\bar{K}$ (Fig. 1). Initial-state-energy positions of the observed structures have been plotted as a function of $\vec{k}_{||}$ (electron momentum parallel to the crystal

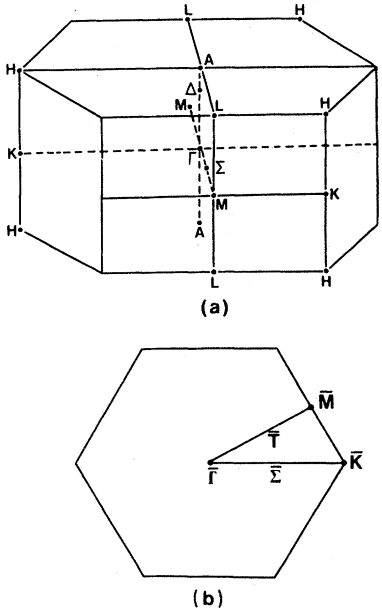

FIG. 1. (a) Bulk Brillouin zone and (b) surface Brillouin zone for a hcp lattice.

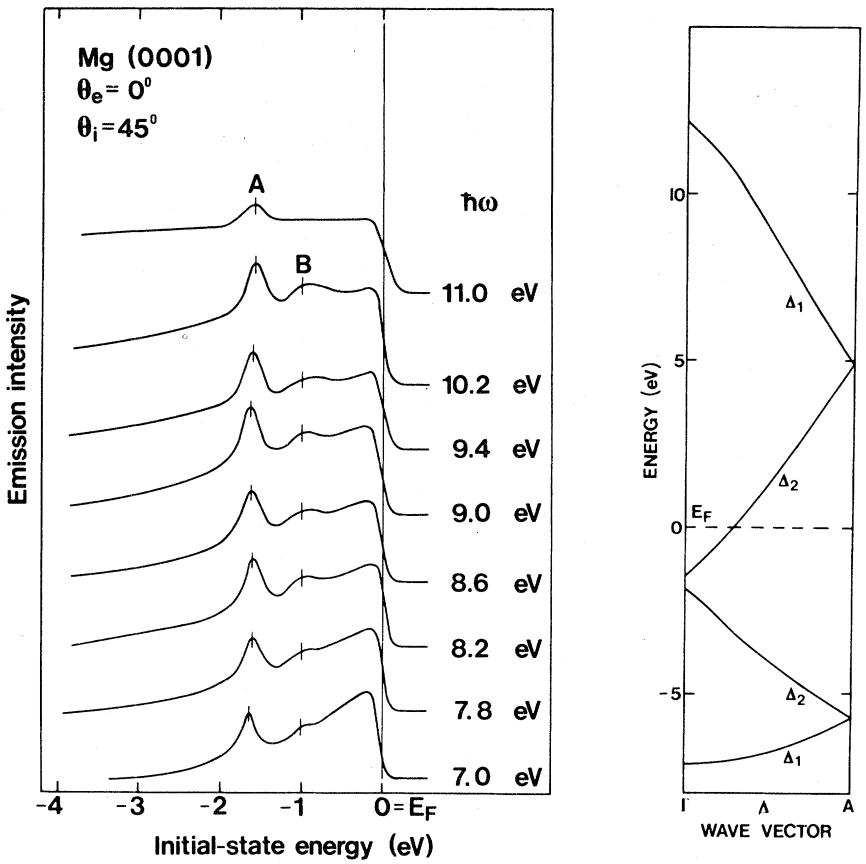

FIG. 2. Experimental AREDC's for photoelectrons emitted normal to the Mg(0001) crystal face for photon energies between 7.0 and 11.0 eV. On the right-hand side is the APW band structure of magnesium along the ΓA symmetry line.

face) to obtain the experimental electron bands. The positions and dispersions of these bands have been compared to both the band gaps obtained by projecting the three-dimensional (3D) band structure from an augmented-plane-wave (APW) calculation onto the SBZ for the (0001) face and to the predicted direct transitions using the same band calculation.

EXPERIMENTAL

The angle-resolved spectra were recorded in two different ARUPS spectrometers. The $\hbar\omega = 16.8$-, 21.2-, and 26.8-eV spectra were measured in a VG ADES 400 system. The low-photon-energy spectra were measured in an ARUPS spectrometer connected to a McPherson 225 monochromator. A hydrogen discharge served as a light source. The monochromator-light source combination produced useful light in the range 7.0—11.6 eV. The emitted electrons were energy analyzed by a movable 180° spherical deflection analyzer with an energy resolution ($\Delta E/E$) of 1.5%. Monochromator slits and analyzer voltages were set to obtain a combined (electron and photon) energy resolution of ≤ 0.3 eV in the recorded spectra.

The sample was a high-purity Mg(0001) single crystal that had been spark cut and mechanically polished. In order to obtain a bright mirrorlike surface the crystal was then electropolished in a solution of one part nitric acid to two parts methyl alcohol at -20 °C.[14] The crystal was cleaned *in situ* by repeated cycles of argon sputtering and annealing. This cleaning procedure produced a clean and intense sixfold symmetric low-energy electron diffraction (LEED) pattern. The LEED pattern was utilized to choose the azimuthal angle of the sample.

RESULTS AND DISCUSSION

Angle-resolved electron distribution curves (AREDC's) for electrons emitted in the normal

direction ($\theta_e = 0°$) from a Mg(0001) crystal surface are shown in Fig. 2 together with the calculated band structure along the ΓA symmetry line in the Brillouin zone. As seen in the figure the two observed structures are at constant initial-state energy, when the photon energy is varied from 7.0 to 11.0 eV. In normal emission the dominant peak (A) is located 1.7 eV below the Fermi edge (E_F) and the smaller structure (B) is at an initial-state energy of -1.1 eV. It should be noted that peak A is weak and peak B cannot be resolved in the $\hbar\omega = 11.0$ eV spectrum. Spectra have also been measured at higher photon energies: 11.6, 16.8, 21.2, and 26.8 eV. The recorded intensity from the Mg valence band was very low in these spectra, but no shifts in the A and B peaks could be detected. The low photoemission cross section is not unexpected. A corresponding drop in intensity near the

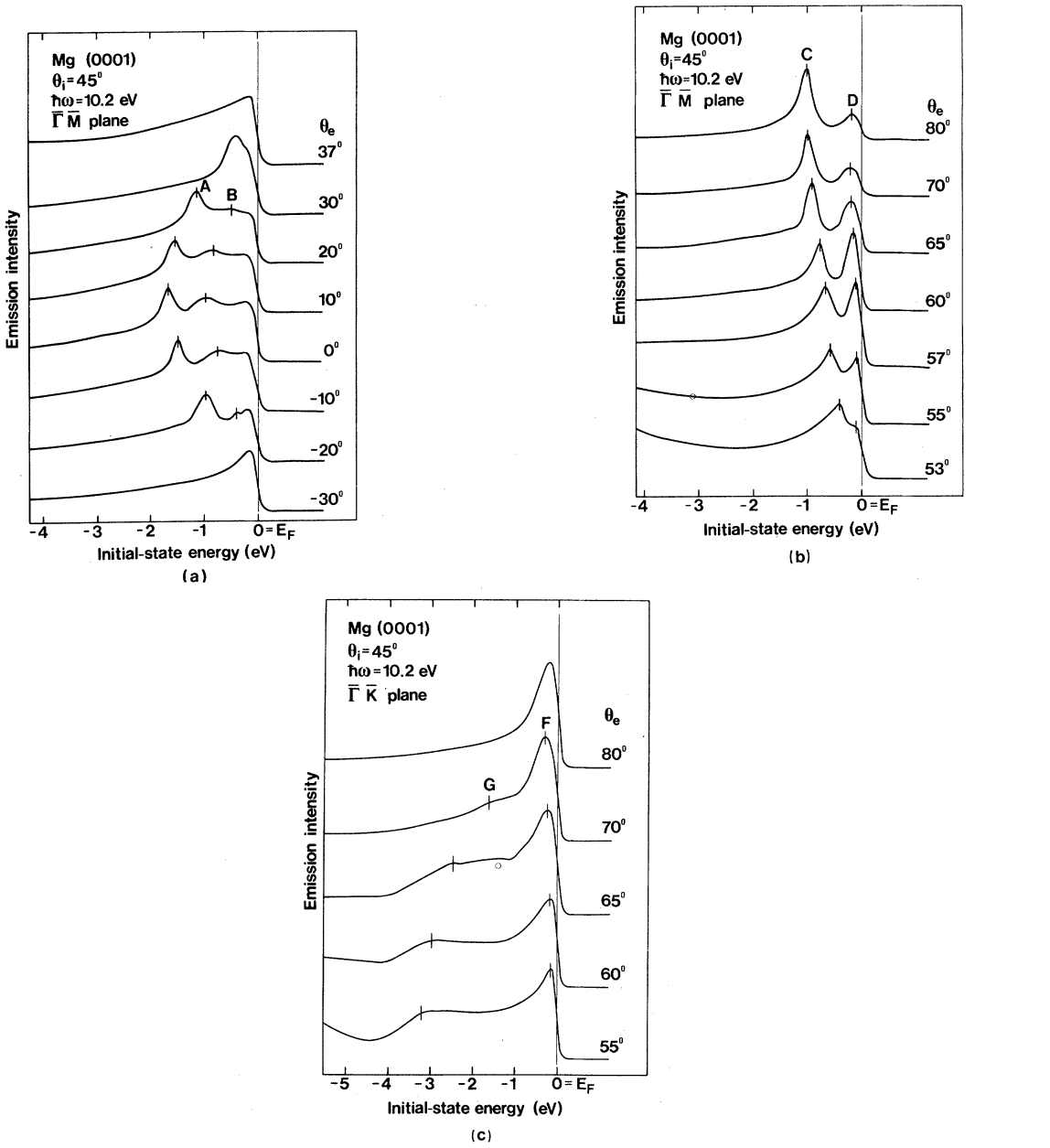

FIG. 3. (a) Experimental AREDC's for Mg(0001) at different polar angles. The polar angle is varied in the ΓALM plane with $\hbar\omega = 10.2$ eV. (b) Same as (a) but for large polar angles. (c) Experimental AREDC's for Mg(0001) as a function of emission angle in the ΓAHK azimuthal direction, $\hbar\omega = 10.2$ eV.

bulk-plasmon energy has been reported for aluminum,[6] and can be understood as it reflects the decrease of the effective vector potential at the surface for photon energies above the bulk-plasmon energy.

The polar-angle dependence of the photoemission was studied in the symmetry planes ΓALM and ΓAHK for different photon energies. Figure 3(a) shows a set of AREDC's for the ΓALM plane using 10.2-eV radiation. Peaks A and B show a strong and symmetric dispersion with respect to ΓA passing E_F at about $\theta_e = 33°$ and 25°, respectively. For large polar angles ($\theta_e \geq 53°$) two new structures, C and D, are observed in the ΓALM plane. The AREDC's for $53° \leq \theta_e \leq 80°$ are shown in Fig. 3(b). As shown in the spectra peak C moves to lower initial-state energies for increasing θ_e, while peak D is constant in initial-state energy within 0.1 eV.

The AREDC's recorded in the ΓAHK plane for $\theta_e \leq 40°$ are similar to the ones shown in Fig. 3(a) for the ΓALM plane concerning peaks A and B. As can be seen in Fig. 3(c) the spectra for $\theta_e \geq 50°$ in the ΓAHK plane are different from the ones for the ΓALM plane. A broad shoulder (G) is observed for $\theta_e \geq 55°$. This shoulder disperses towards E_F for increasing θ_e until $\theta_e = 70°$ and is not observed for $\theta_e = 80°$. For $\theta_e = 55°$ a sharp peak (F) is observed 0.1 eV below E_F. This peak shows a weak dispersion away from the Fermi edge for increasing θ_e.

In order to study the polarization dependence of the structures, the angle of light incidence (θ_i) was varied. In Fig. 4 spectra recorded at $\theta_e = 60°$ and $\theta_e = 15°$ for $\theta_i = 45°$ (mixed s and p polarization) and $\theta_i = 0°$ (no A component normal to the surface) are shown. As indicated in the figure both peaks A and C show a decreasing intensity for small θ_i.

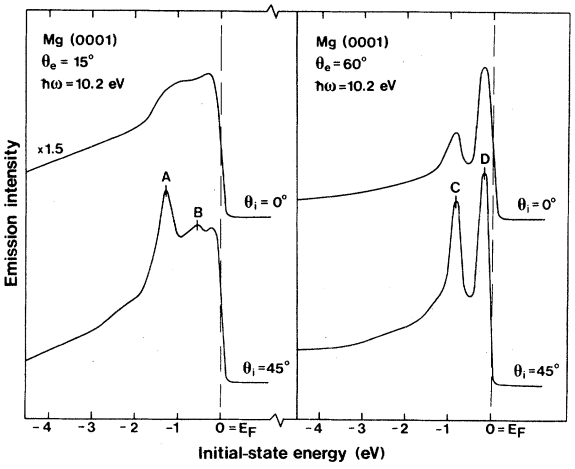

FIG. 4. (a) Experimental AREDC's at $\theta_e = 15°$ for $\theta_i = 45°$ and $\theta_i = 0°$ and (b) at $\theta_e = 60°$ for the same pair of angles of light incidence. Photon energy is 10.2 eV and the photoelectrons are analyzed in the ΓALM azimuthal direction.

The positions in initial-state energy (E_i) of the three peaks A, B, and C as a function of $\vec{k}_{||}$ are summarized in Fig. 5(a). We plot $E_i(\vec{k}_{||})$ along the $\bar{\Gamma}\bar{M}$ and $\bar{\Gamma}\bar{K}$ lines; the shaded area is the projection of the 3D band structure of Mg onto the SBZ of the (0001) surface. We observe that peak A is located in a band gap opening up at $\bar{\Gamma}$, similarly

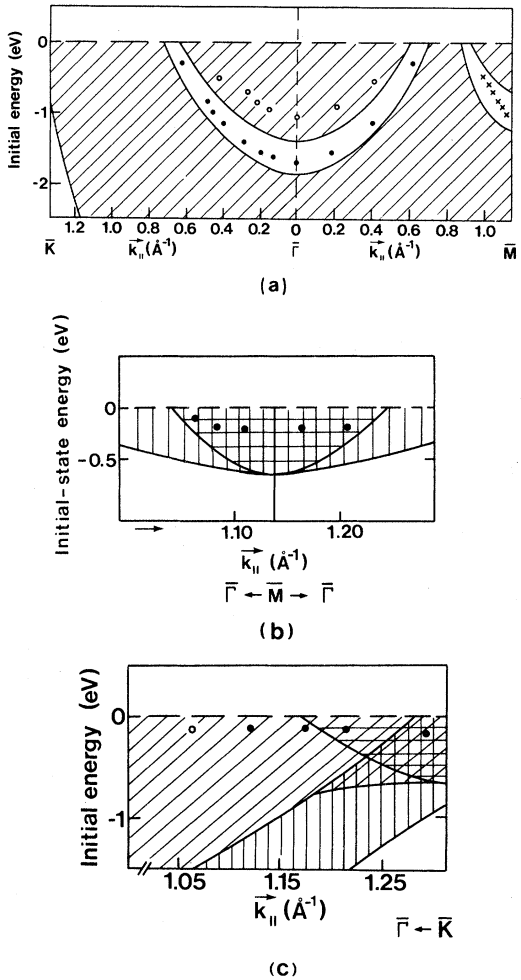

FIG. 5. (a) Dispersions of peak A (dots), peak B (rings), and peak C (crosses). Unhatched areas show the band gaps. (b) Initial-state energy of peak D for different $\vec{k}_{||}$. Vertically hatched area shows the projection of the third band and horizontally hatched area shows the projection of the fourth band. (c) Initial-state energy of peak F for different $\vec{k}_{||}$. Vertically, diagonally, and horizontally hatched areas show the projections of the first, second, and third bands, respectively.

peak C is located in a band gap at $\bar{M}$. Both peaks A and C show dispersions $E_i(\vec{k}_{||})$ that nicely fall within the band gaps. In Fig. 5(b) E_i for peak D is plotted as function of $\vec{k}_{||}$, together with the projection of the bands around the $\bar{M}$ point. For peak F, $E_i(\vec{k}_{||})$ is plotted in Fig. 5(c), also drawn is the projection of the bands in the vicinity of the $\bar{K}$ point.

In order to interpret a structure as emission from a surface state it is necessary that its initial-state energy is constant for normal emission, when the photon energy is varied. The energy position of the structure should also be within a gap of the projected bulk bands. Most surface states detected are also only excited by p-polarized light, but there are no absolute arguments prohibiting excitation with s-polarized light. The sensitivity to the light polarization is coupled both to the symmetry of the surface state and to the excitation mechanism. The symmetry of the surface state is given by the bulk bands enclosing the band gap.[15] Assuming dipole transitions caused by bulk potentials, the selection rules are valid for both bulk and surface states.[16] If the excitation mechanism is tied to the surface discontinuity (surface potential gradient or excitation field gradient), we will necessarily need p-polarized light for the excitation of any initial state independent of its symmetry. An analysis similar to the one in Ref. 16 shows that for surface photoemission only symmetrical initial states, i.e., Δ_1 and Δ_2 states can be excited in normal emission from hcp elements.

For peak A the symmetry Δ_2 will prevent excitation by s-polarized light independent of excitation mechanism for $\theta_e = 0°$ in agreement with the spectra in Fig. 4(a). Peak C is observed only in off-normal emission where we cannot assign a definite symmetry to it, but the polarization dependence seen in Fig. 4(b) could be assigned to surface photoemission as being the excitation mechanism.

We have observed six main features in the AR-UPS spectra, and according to the surface-state criteria discussed above we interpret two, A and C, as emission from surface states. We assign peak A to be emission from a surface state located in the band gap at $\bar{\Gamma}$. Similarly we interpret peak C as emission from a surface state in the $\bar{M}$ band gap [Fig. 5(a)].

Peak B we assign to be surface photoemission from the upper of the two Δ_2 bands enclosing the peak A surface-state band gap. The interpretation of peak B as a reflection of the initial bulk density of states probed by surface photoemission is supported by its stability in initial-state energy for all photon energies used. Furthermore when its initial-state energy is plotted as a function of $\vec{k}_{||}$, the dispersion displays a similar shape to the calculated band edge and the absolute energy positions are within 0.15 eV [Fig. 5(a)]. If peak B reflects states near the upper band edge, the obvious question arises, why is not the high density of states near the lower band edge observed? One possible explanation is that the lower band edge is too smeared out due to lifetime effects. This depends critically on how much of the total charge in the surface layer is carried by the surface state A. It should also be noted that the charge redistribution between the surface state and the lower band edge is under discussion. For Cu(111) it is suggested that there is a charge transfer in the surface layers from the sp band to the surface state,[17] which would weaken the emission from the lower band edge.

We assign peak D to be emission from the electron pocket around the L point, $\bar{M}$ point in the SBZ [see Fig. 5(b)]. Around this point the third and the fourth bands dip below the Fermi energy and give a flat band region. This region with a high density of occupied states have been observed before in both magnetoacoustic attenuation and de Haas–van Alphen experiments.[18,19] The position of the calculated final state bands are also in favor of a high photocurrent, since we are close to a direct transition.

The band structure near the K-H line in the bulk Brillouin zone is quite complex. The projection of the three lowest bulk bands numbered one to three with increasing energy near the K point in the SBZ are drawn in Fig. 5(c) together with the experimental energy positions of the peak F. As seen in the figure our data points extend outside the theoretical third band, but the largest signal-to-background ratio is obtained when we probe within the calculated third-band electron pocket.

For emission $\theta_e = 80°$ in the ΓAHK plane we probe states close to the Brillouin-zone boundary. In a free-electron picture, the electron bands are threefold degenerate along the K-H line. We assign the high intensity in the $\theta_e = 80°$ spectrum to a direct transition between a very flat threefold degenerate initial-state band and an also threefold degenerate final-state band.

For smaller emission angles ($\theta_e < 80°$) in the ΓAHK plane, we can distinguish two structures, F and G [Fig. 3(c)]. We believe that peak F reflects the flat band region of bands 2 and 3 near the K point, $\bar{K}$ point in the SBZ. Theoretically, part of the intensity could originate from a direct transi-

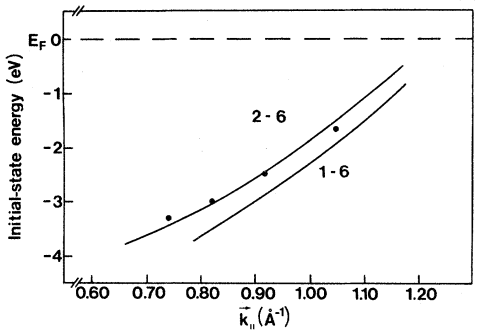

FIG. 6. Comparison between the experimental and calculated positions of peak G as a function of $\vec{k}_{\parallel}$ in the ΓALM plane. The upper line corresponds to a direct transition between bands 1 and 6.

tion between bands 2 and 8 near the H point. The contribution from this transition must be very small, since this is emission into a secondary cone.[20] The shoulder G we assign to be a direct transition between bands 2 and 6 as seen in primary cone emission. In Fig. 6 the experimental positions of G are compared to the theoretical positions of direct transitions between bands 1 and 6 and between bands 2 and 6.

CONCLUSIONS

The work presented in this paper shows clear evidence of photoemission from two surface states on the (0001) surface of Mg. One of them, A, is located in the band gap at $\bar{\Gamma}$; the other, C, in the band gap at $\bar{M}$. Both surface states have been found to be more sensitive to oxygen contamination than the other structures observed in the spectra. However they do not show extreme sensitivity to gas adsorption, since they are detectable even after exposure of 50 L of oxygen. This can be understood since both surface states are located in fairly narrow band gaps, which means that the wave functions of the surface states will therefore be rather insensitive to changes of the surface potential.

We have also observed photoemission from three different regions in the Brillouin zone with high densities of states. These electron pockets are found near Γ, L, and K. The one located around Γ, peak B in the spectra (see Fig. 2), has been detected in normal emission for photon energies in the range 7.0—26.8 eV. The parameters determining the strength of these indirect transitions are not fully understood. Clearly the photon energy is important, but also the polarization of the light will effect the spectra as seen in Fig. 4. Indirect transition from band edges have also been reported from Al(100) (Ref. 4) and Zn(0001) (Ref. 21). Structures D and F confirm magnetoacoustic attenuation and de Haas—van Alphen experiments[18,19] with respect to the electron pockets around L and K.

Of the six features observed in the spectra, five are sharp peaks. The remaining one, G, is a broad shoulder. This indicates an origin different from the other five structures. We have assigned this shoulder to a direct transition. It can be noted that the direct transitions found in Zn (Ref. 21) and Al (Refs. 11 and 12) are also very broad compared to the surface-state contributions.

ACKNOWLEDGMENT

This work was supported in part by the Swedish Natural Science Research Council.

[1]P. J. Feibelman, Phys. Rev. Lett. 34, 1092 (1975); Phys. Rev. B 15, 1219 (1975).
[2]K. L. Kliewer, Phys. Rev. B 14, 1412 (1976); 15, 3759 (1977).
[3]J. B. Pendry and J. F. L. Hopkinson, J. Phys. (Paris) C 4, 142 (1978).
[4]P. O. Gartland and B. J. Slagsvold, Solid State Commun. 25, 489 (1978).
[5]G. V. Hansson and S. A. Flodström, Phys. Rev. B 18, 1562 (1978).
[6]H. J. Levinson, E. W. Plummer, and P. J. Feibelman, Phys. Rev. Lett. 43, 952 (1979); H. J. Levinson and E. W. Plummer, Phys. Rev. B 2, 628 (1981).
[7]E. B. Caruthers, L. Kleinman, and G. P. Alldredge, Phys. Rev. B 8, 4570 (1973); 9, 3325 (1974); 9, 3330 (1974).
[8]J. R. Chelikovsky, M. Schlüter, S. G. Louie, and M. L. Cohen, Solid State Commun. 17, 1103 (1979).
[9]Ding-Sheng Wang, A. J. Freeman, H. Krakauer, and M. Posternak, Phys. Rev. B 23, 1685 (1981).
[10]K. Mednick and L. Kleinman, Phys. Rev. B 22, 5768 (1980).
[11]J. K. Grepstad and B. J. Slagsvold (unpublished).
[12]U. O. Karlsson, G. V. Hansson, and S. A. Flodström (unpublished).
[13]S. A. Flodström and C. W. B. Martinsson (unpublished).
[14]H. Modin and S. Modin, in *Handbok i Metallmikroskopering* (Meritförlaget, Stockholm, 1968).

[15]J. B. Pendry, private communication.
[16]J. Hermansson, Solid State Commun. 22, 9 (1977).
[17]Y. Petroff and P. Thiry, Appl. Opt. 19, 3957 (1980).
[18]J. B. Ketterson and R. W. Stark, Phys. Rev. 156, 748 (1967).
[19]R. W. Stark, Phys. Rev. 162, 589 (1967).
[20]G. D. Mahan, Phys. Rev. B 2, 4334 (1970).
[21]F. J. Himpsel, D. E. Eastman, and E. E. Koch, Phys. Rev. B 24, 1687 (1981).